THE JOURNAL OF PHYSICAL CHEMISTRY B

Article

pubs.acs.org/JPCB

Water Dynamics in Water/DMSO Binary Mixtures

Daryl B. Wong, Kathleen P. Sokolowsky, Musa I. El-Barghouthi,[†] Emily E. Fenn,[‡] Chiara H. Giammanco, Adam L. Sturlaugson, and Michael D. Fayer*

Department of Chemistry, Stanford University, Stanford, California 94305, United States

ABSTRACT: The dynamics of dimethyl sulfoxide (DMSO)/water solutions with a wide range of water concentrations are studied using polarization selective infrared pump−probe experiments, two-dimensional infrared (2D IR) vibrational echo spectroscopy, optical heterodyne detected optical Kerr effect (OHD-OKE) experiments, and IR absorption spectroscopy. Vibrational population relaxation of the OD stretch of dilute HOD in H_2O displays two vibrational lifetimes even at very low water concentrations that are associated with water−water and water−DMSO hydrogen bonds. The IR absorption spectra also show characteristics of both water−DMSO and water−water hydrogen bonding. Although two populations are observed, water anisotropy decays (orientational relaxation) exhibit single ensemble behavior, indicative of concerted reorientation involving water and DMSO molecules. OHD-OKE experiments, which measure the orientational relaxation of DMSO, reveal that the DMSO orientational relaxation times are the same as orientational relaxation times found for water over a wide range of water concentrations within experimental error. The fact that the reorientation times of water and DMSO are basically the same shows that the reorientation of water is coupled to the reorientation of DMSO itself. These observations are discussed in terms of a jump reorientation model. Frequency−frequency correlation functions determined from the 2D IR experiments on the OD stretch show both fast and slow spectral diffusion. In analogy to bulk water, the fast component is assigned to very local hydrogen bond fluctuations. The slow component, which is similar to the slow water reorientation time at each water concentration, is associated with global hydrogen bond structural randomization.

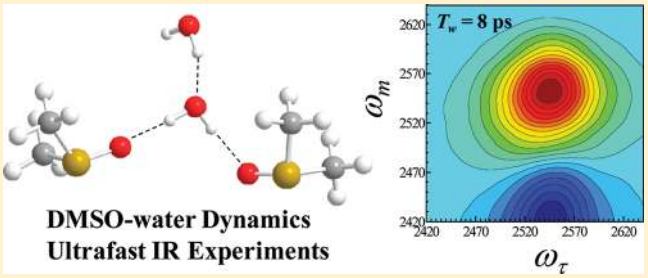

I. INTRODUCTION

Here we present a comprehensive examination of the dynamics and interactions of water in mixtures of water and dimethyl sulfoxide (DMSO). Solutions are studied that range from very low water content to high water content. Five experimental observables are employed. The techniques, which are all applied as a function of water concentration, are infrared (IR) absorption spectra of the water hydroxyl stretch, IR pump−probe experiments that measure the hydroxyl stretch vibrational lifetimes, polarization selective IR pump−probe experiments that measure the water orientational relaxation times, two-dimensional IR (2D IR) vibrational echo experiments that measure spectral diffusion of the hydroxyl stretch, and optical heterodyne detected optical Kerr effect (OHD-OKE) experiments that measure the orientational relaxation of DMSO. By combining the results of these methods, a detailed picture of the nature of water/DMSO dynamics and interactions is obtained, which in turn increases our understanding of how water behaves in complex environments.

The structure and fast dynamics of water's hydrogen bond network are responsible for its unique physical properties such as its increase in volume upon freezing, large heat capacity, and its density maximum at 277 K.[1,2] The rapid rearrangement of the network of hydrogen bonds is responsible for water's extraordinary ability to solvate charges and support biological activity.[3] When water interacts with ions,[4−8] neutral molecules,[9,10] or interfaces,[11−13] its hydrogen bond network structure and dynamics deviate from those of bulk water. There are many instances in which water is found in mixed systems where it is either the major or minor component. Therefore, it is desirable to gain insight into differences in water's hydrogen bond dynamics as a system changes from water poor to water rich.

The infinite miscibility of DMSO with water at room temperature makes water/DMSO solutions useful for gaining insight into changes in water hydrogen bond dynamics as water goes from a minor component to a major component of the solutions. While water is both a hydrogen bond donor and acceptor, DMSO is only a hydrogen bond acceptor. This difference gives rise to a variety of important properties of water/DMSO binary solutions. Solutions of water/DMSO form a eutectic in molar ratios of 2:1 and at low DMSO concentrations serves as a cryoprotectant with a depressed freezing point of 203 K.[14,15] At mole fractions of 0.3−0.4 DMSO, water/DMSO solutions deviate strongly from ideality, with positive deviations in viscosity[16,17] and density and negative deviations in the heat of mixing.[17,18] These distinctive characteristics have inspired a host of studies which have examined the structure and dynamics of these binary mixtures.

Received: February 28, 2012
Revised: April 13, 2012
Published: April 17, 2012

 © 2012 American Chemical Society dx.doi.org/10.1021/jp301967e | *J. Phys. Chem. B* 2012, 116, 5479−5490

Neutron scattering,[19,20] vibrational spectroscopy,[21,22] dielectric spectroscopy,[23] and MD simulations[24,25] have shed light on the structure of water/DMSO. DMSO/water solutions above and below a molar ratio of ∼1:1 consist of different dominant structures. In solutions with greater than 50% DMSO (low water concentration), water will generally hydrogen bond by bridging two DMSO oxygens,[21,25] but there will also be some water−water hydrogen bonds that increase in number as the water concentration is increased. In solutions with DMSO concentrations less than 50%, water will have a tetrahedral hydrogen bond structure, but DMSO oxygens will act as hydrogen bond acceptors for water hydroxyls replacing some water oxygens that would be the acceptors in pure water. In the water-rich solutions, the tetrahedral structure around water molecules leads to local structures with ratios of 1 DMSO to 2 waters, although MD simulations have also shown evidence of 2 DMSOs to 3 waters.[26] Though one type of structure (bridging vs tetrahedral) tends to dominate above or below 50% DMSO, the structures described coexist to some extent, especially in solutions of intermediate concentration.[25] Additionally, water is reported to have little hydrophobic interactions with the methyl groups of DMSO[20] but is reported to form stronger hydrogen bonds with DMSO's oxygen than with water's oxygen.[27]

Although a consensus structure of water/DMSO solutions has been formulated, a consistent picture of the water's dynamics in solution does not yet exist. NMR[27−29] and dielectric relaxation[23] experiments exhibit rotational time constants with a significant slowing of rotational motion when compared with bulk water. However, quasi-elastic neutron scattering (QENS)[30]and Raman-induced Kerr effect spectroscopy (RIKES)[31] report fast water rotational times of ∼1 ps, faster than that of bulk water 2.6 ps.[11] Each measurement has potential difficulties determining water dynamics. Dielectric relaxation, QENS, and NMR measurements require fits of line shapes or indirect decays (spin−lattice relaxation) to multiple parameters, extracting averaged orientational dynamics. RIKES, though an ultrafast technique, relies on the molecular polarizability for signal, and the anisotropic polarizability of DMSO is much larger than that of water and therefore has trouble directly probing water's dynamics.[31]

In the following study, we use polarization selective pump−probe experiments, 2D IR vibrational echo spectroscopy, and IR absorption spectroscopy to observe the OD stretch of dilute HOD in H_2O/DMSO solutions. The OD stretch of dilute HOD in H_2O/DMSO mixtures is studied for several reasons. The OD hydroxyl stretch is a local mode, which simplifies the spectrum by eliminating overlapping symmetric and antisymmetric stretches that arise for H_2O. In addition, studying the dilute OD hydroxyl stretch eliminates vibrational excitation transfer,[32,33] which interferes with both the pump−probe and vibrational echo observables. Simulations of bulk water have shown that dilute HOD does not change water's dynamics and that the OD hydroxyl stretch reports on the dynamics of the overall water hydrogen bond network.[34]

The results of vibrational lifetime measurements indicate that even at very low water concentration there are both water−water hydrogen bonds and water−DMSO hydrogen bonds, which is in accord with the IR absorption spectra. The polarization selective IR pump−probe experiments demonstrate that for solutions with water concentrations as high as 1 DMSO:4 waters, water reorients as one collective ensemble after fast, local orientational diffusive motion (wobbling-in-a cone[11,35−37]), in spite of the two water populations indicated by the two vibrational lifetimes. The OHD-OKE experiments, which measure the DMSO orientational relaxation because DMSO has a much larger anisotropic polarizability than water, show that the slow component of the water orientational relaxation is tied to DMSO orientational relaxation. The 2D IR vibrational echo measurements of spectral diffusion display water structural dynamics on multiple time scales.[5,38,39] In analogy to bulk water, the very fast dynamics are assigned to very local hydrogen bond fluctuations, while the slowest component of the spectral diffusion arises from complete structural randomization of the water/DMSO system.

II. EXPERIMENTAL PROCEDURES

A. Sample Preparation. DMSO (Acros Organics), D_2O (Acros Organics), and H_2O (Fisher Scientific) were used as received. Resonant and nonresonant solutions with molar ratios of n = 18:1, 9:1, 5:1, 2:1, 1:1, 1:2, 1:4, and 1:9 DMSO:water were made, where resonant solutions contained 5% HOD in H_2O and nonresonant solutions contained only H_2O. Water content was confirmed by Karl Fischer titration. The thickness of each sample is chosen to achieve an absorbance of ∼0.5 for pump probe experiments and ∼0.2 for vibrational echo experiments at the peak of the OD stretch absorption.

B. Vibrational Spectroscopy. Linear FT-IR spectra were acquired on a Thermo Nicolet 6700 FT-IR at 2 cm^{-1} resolution. The ultrafast infrared experiments were performed using a laser system described previously. It produces horizontally polarized ∼70 fs mid-infrared pulses with a fwhm of 220 cm^{-1}.[40] The mid-IR pulse center frequency was tuned from ∼2550 cm^{-1} in the sample with lowest water concentration to 2511 cm^{-1} in the sample with the highest water concentration so that the center of the mid-IR spectrum is matched to the peak of the OD absorption to ensure even excitation across the OD absorption band.

1. Pump−Probe Experiments. Vibrational lifetime and anisotropy experiments were conducted by splitting the mid-infrared pulse into a strong (∼90%) pump and a weak (∼10%) probe pulse. The pump pulse polarization was rotated to 45° with respect to the laboratory frame by a half-wave plate and followed by a thin film polarizer oriented at 45° immediately before it interacted with the sample, ensuring linear polarization. The probe pulse, after passing through the sample, was resolved parallel and perpendicular with respect to the pump. The probe was frequency dispersed in the monochromator and detected using a 32-element HgCdTe (MCT) array detector.

The signals, which track the temporal decay of the probe parallel ($I_{\parallel}$) and perpendicular ($I_{\perp}$) to the pump pulse, contain information about both the population and orientational dynamics.[41]

$$I_{\parallel} = P(t)(1 + 0.8C_2(t)) \tag{1}$$

$$I_{\perp} = P(t)(1 - 0.4C_2(t)) \tag{2}$$

$P(t)$ is the vibrational population, and $C_2(t)$ is the second Legendre polynomial correlation function (orientational correlation function) of the OD mode. Population relaxation is obtained by combining the parallel and perpendicular signals:

$$3P(t) = I_{\parallel} + 2I_{\perp} \tag{3}$$

In addition, the two resolved signals can also be used to extract the anisotropy $r(t)$, which is related to the orientational correlation function

$$r(t) = \frac{I_{\parallel} - I_{\perp}}{I_{\parallel} + 2I_{\perp}} = 0.4C_2(t) \quad (4)$$

2. 2D IR Vibrational Echo Experiment. Details of the methods and analysis of the 2D IR experiment have been described in detail previously.[40,42] Briefly, the infrared pulse is split into three excitation pulses which interact with the sample, which generates the vibrational echo pulse, and into a fourth pulse, which serves as a local oscillator (LO). The vibrational echo is optically heterodyned with the LO, frequency dispersed by a monochromator, and measured with a 32-element MCT array. Several blocks of 32 frequencies detected by the array give the ω_m axis of the 2D IR spectrum (vertical, frequency of echo emission). The signal on a given pixel produces a temporal interferogram as τ, the time between the first and second pulses in the pulse sequence, is scanned. The temporal interferograms are Fourier transformed to give the ω_τ axis of the 2D IR spectrum (horizontal axis, frequency of pulse 1's radiation field-oscillator interaction). The dynamical information is contained in the change in shape of the 2D IR spectra as T_w, the time between the second and third pulses, is changed.

The time dependence of the 2D IR spectra yields the spectral diffusion, which is caused by the structural evolution of the system. The time scales and amplitudes of the frequency changes are obtained from the 2D IR spectra by constructing the frequency−frequency correlation function (FFCF). The FFCF is obtained from the T_w-dependent 2D IR spectra using center line slope (CLS) analysis.[43,44] Simultaneous fitting of the CLS and the linear absorption spectrum provides the parameters for the FFCF. The FFCF is the joint probability that a vibrational oscillator with a particular frequency at $t = 0$ will still have the same frequency at a later time t averaged over all initial frequencies. The decay of the FFCF is caused by structural changes in the system and is used to determine different time scales of structural evolution.

The FFCF can be described by a sum of exponential decays

$$C_1(t) = \langle \delta\omega_{1,0}(\tau)\delta\omega_{1,0}(0)\rangle = \sum_i \Delta_i^2 \exp(-t/\tau_i) \quad (5)$$

where the Δ_is are the amplitudes of the frequency fluctuations of each component and the τ_is are the associated time constants. The τ_i values are the decay times and reflect the time scales associated with the structural fluctuations. Δ_is are the values of the standard deviation of a Gaussian line shape and represent the amplitude of the frequency fluctuations associated with the corresponding τ_i. If $\Delta\tau < 1$, this component of the frequency fluctuations is motionally narrowed (homogeneous broadening), and Δ and τ cannot be determined separately. The motionally narrowed homogeneous contribution to the absorption spectrum has a pure dephasing width given by $\Gamma^* = \Delta^2\tau = 1/\pi T^*_2$, where T^*_2 is the pure dephasing time and Γ^* is the pure dephasing line width. The homogeneous line width is dominated by pure dephasing, but the observed homogeneous dephasing time, T_2, also has contributions from the vibrational lifetime and orientational relaxation

$$\frac{1}{T_2} = \frac{1}{T^*_2} + \frac{1}{2T_1} + \frac{1}{3T_{or}} \quad (6)$$

where T^*_2, T_1, and T_{or} are the pure dephasing time, vibrational lifetime, and orientational relaxation time, respectively. The total homogeneous line width is $\Gamma = 1/\pi T_2$. The total inhomogeneous line width is the convolution of the Δs. Multiplying the convolution by 2.35 gives the full width at half-maximum (fwhm) of the total inhomogeneous line width. Γ is the width (fwhm) of the homogeneous contribution to the absorption line. The total absorption line is the convolution of total inhomogeneous fwhm with Γ.

3. OHD-OKE Spectroscopy. The details of the laser and spectrometer used in the OHD-OKE experiment have been described in detail elsewhere.[45] The following is a brief summary. Pulses at 800 nm were generated from a Ti:sapphire mode-locked oscillator seeded 5 kHz Ti:sapphire regenerative amplifier. The optical Kerr effect is a nonresonant pump−probe technique in which a linearly polarized (0°) pump laser pulse induces a transient birefringence in a liquid sample. A second, linearly polarized (45°) pulse probes the sample, emerging elliptically polarized due to the pump-induced birefringence in the sample. The decay of the birefringence is measured by varying the pump−probe delay and is related to the orientational relaxation dynamics of the liquid. Heterodyne detection and phase cycling improve the signal-to-noise ratio in the experiments.[45]

III. RESULTS AND DISCUSSION

A. Infrared Absorption Spectroscopy. The linear absorption spectra of the OD stretch of dilute HOD in water/DMSO mixtures at various concentrations are shown in Figure 1. The positions of the peak maxima and the full width at half-maximum height (fwhm) obtained from Gaussian fits to the spectra reflect changes in the hydrogen bonding structure as the water concentration is varied. While the line shapes are not perfect Gaussians, the fits nonetheless reflect the changes with water concentration. The results of the fits are given in Table 1.

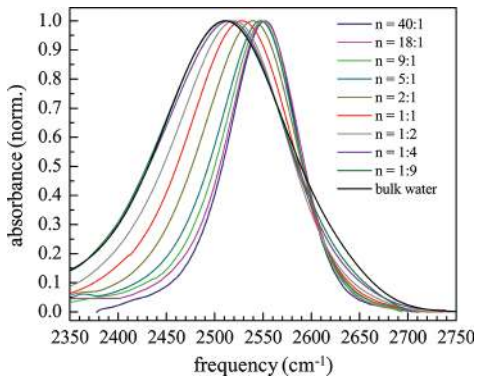

Figure 1. Linear FT-IR spectra of the OD stretch of dilute HOD in water−DMSO solutions. n is the number of DMSO molecules to water molecules, DMSO:water. As the water concentration increases, the line broadens and shifts to lower frequency.

Table 1. Peak maxima and FWHM of Gaussian Fits to Linear Absorption Spectra of the OD Stretch of Water in DMSO as a Function of Molar Ratio

DMSO:water	peak max (cm^{-1})	fwhm (cm^{-1})	DMSO:water	peak max (cm^{-1})	fwhm (cm^{-1})
40:1	2551	83	1:1	2526	122
18:1	2551	87	1:2	2518	132
9:1	2547	88	1:4	2512	150
5:1	2546	93	1:9	2511	156
2:1	2538	106	bulk water	2511	162

dx.doi.org/10.1021/jp301967e | J. Phys. Chem. B 2012, 116, 5479−5490

As the water concentration increases, the peak red shifts (absorption at longer wavelength) from ~2550 cm^{-1} at the lowest water concentration (n = 40:1 DMSO:water) to nearly that of bulk water at X = 0.9 (n = 1:9 DMSO:water). X is the mole fraction of water, and n is the number of DMSO molecules to the number of water molecules.

Attempts were made to fit the intermediate concentration spectra as a sum of the lowest water concentration spectrum (n = 40:1) to reflect water−DMSO hydrogen bonds and the bulk water spectrum representing water−water hydrogen bonds. However, the total spectrum could not be fit as the sum of two spectra that only change amplitude as the amount of water is changed. This shows that the nature of the hydrogen bond network changes as the water concentration changes.

In systems containing water, the absorption frequency of a hydrogen bond donating hydroxyl stretch is a sensitive probe of local hydrogen bond strengths and molecular environments.[2,46−48] The stronger the hydrogen bond, the greater the red shift.[46] Bulk water's very broad line width is caused by a wide range of hydrogen bond strengths, with strong hydrogen bonds absorbing on the red side of the line and weak hydrogen bonds absorbing on the blue side of the line.[47] Much of the broadening and shift of the spectra (Figure 1) with an increase of water content in the water/DMSO mixtures is caused by an increased number of water−water hydrogen bonds.

At lowest water contents, in addition to being blue-shifted the lines are very narrow relative to the bulk water spectrum. As the concentration of water is increased, there is simultaneous red shifting of the peak center and broadening on both red and blue sides. The broadening on both sides of the low water concentration spectrum indicates that there are an increasing number of water−water hydrogen bonds, which have a wider range of hydrogen bond strengths than water−DMSO hydrogen bonds. The broadening on the blue side of the line occurs at all water concentrations but becomes pronounced above n = 1:1. Significantly increased spectral broadening above n = 1:1 implies that further increases in water concentration lead to an increase in the number and diversity of water−water and water−DMSO interactions.

As mentioned in the Introduction, MD simulations of water/DMSO solutions with water concentrations up to 1:1 molar ratios[25] mainly observe structures involving 2 DMSO oxygens bridged by 1 water molecule. A narrow infrared absorption peak agrees with this observation as much of the water is constrained to bridging hydrogen bond geometries at low water concentration. However, the 1:1 spectrum is much broader than the 40:1 spectrum (see Figure 1), which demonstrates that the addition of water at low water concentration does not simply produce more pairs of DMSO bridged by a single water molecule. The spectra show that even at low water concentrations some water−water hydrogen bonds exist. In solutions with water concentration greater than n = 1:1, studies[23−25] have found that the majority of interactions consist of hydrogen bond structures in which DMSO can act as a surrogate hydrogen bond acceptor in water's tetrahedral structure. However, because the absorption spectrum of samples n = 1:1 and n = 1:2 are not as broad as bulk water, the spectra indicate less variety in hydrogen bond strengths between water and DMSO than the range of water−water interactions found in bulk water. In the discussion of dynamics given below it is important to note that both water−water interactions and water−DMSO interactions exist in all of the binary mixture concentrations studied.

The absorption spectra of water/DMSO show that at lowest water concentration the peak center is blue-shifted by 40 cm^{-1} relative to that of bulk water, which as mentioned above, means the water−DMSO hydrogen bond is weaker than a water−water hydrogen bond. However, previous studies on the system indicate that the water−DMSO hydrogen bond is stronger than the water−water hydrogen bond.[23,27,30,31] While a phenomenon called the improper blue shift of hydrogen bonds[49−51] where a stronger hydrogen bond blue-shifts an IR absorption band exists, the nature of the improper blue-shift is such that the reported cases involve only hydrogen bond donors that are not highly polar (such as C−H). Improper blue-shifting of hydroxyl donors has not been observed.[51] Therefore, following the work of previous infrared studies, we use the conventional interpretation of hydrogen bond strengths and vibrational stretching frequencies to conclude that the observed blue-shift of water−DMSO hydrogen bonds is an indication that the water hydrogen bond to DMSO is weaker than a water−water hydrogen bond.

B. Vibrational Lifetimes. Vibrational relaxation requires the initially excited mode (OD stretch) to deposit its energy into a combination of other modes so that energy is conserved. These are lower frequency molecular vibrations, such as bends, as well as intermolecular modes such as torsions and bath modes.[52] The rate of vibrational relaxation depends on coupling of the OD stretch to the accepting modes and the density of states of the accepting modes.[53,54] The couplings and the density of states are very sensitive to the local environment of the OD hydroxyl, and therefore, differences in the vibrational relaxation rates correspond to differences in local structures.

Figure 2 shows the population relaxation data for a range of DMSO:water concentrations. The vibrational lifetime of each

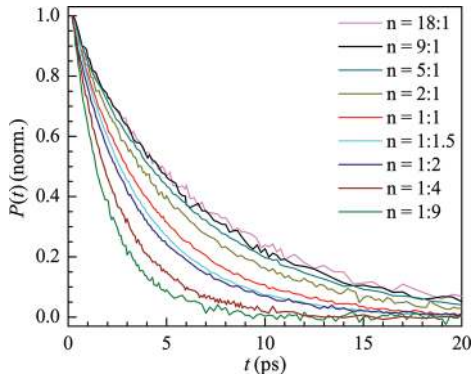

Figure 2. Population relaxation curves, $P(t)$, for various concentrations of DMSO:water measured at the frequency 2520 cm^{-1}.

DMSO:water solution at varying wavelengths across the spectrum fit well to biexponential decays of the form

$$P(t) = A_1 e^{-t/\tau_1} + A_2 e^{-t/\tau_2} \quad (7)$$

The A_i are the fractional population amplitudes. However, the data can also be fit well to single-exponential decays. The fits with the biexponential form yield somewhat better fits, but there is an extra adjustable parameter. To test which model is better, a method called the Akaike information criterion was used.[55] For the single-exponential fit, there are two adjustable parameters: the amplitude and the time constant. For the biexponential fit, there are three adjustable parameters. One of the time constants was fixed and set equal to the vibrational

dx.doi.org/10.1021/jp301967e | J. Phys. Chem. B 2012, 116, 5479−5490

lifetime of the OD stretch when the OD is hydrogen bonded to a water oxygen. This value is 1.8 ps;[11] it is the same in bulk water and in other situations such as very small AOT reverse micelles in which most water hydroxyls are hydrogen bonded to sulfonate head groups, but a small fraction are bonded to water oxygens.[12] Even without fixing the short time component to 1.8 ps, the value of the shorter time constant obtained from fits is still close to 1.8 ps. The results of the Akaike analysis showed that the biexponential fit is unquestionably far superior. Further motivation for biexponential fitting comes from studies such as MD simulations which reveal there are water−DMSO and water−water hydrogen bonds even at low water concentrations.[25] In addition, water in AOT reverse micelles of low water content exhibit similar two population behavior, where the two lifetimes are interpreted as water hydroxyl−water hydrogen bond interactions and the water hydroxyl−sulfonate headgroup hydrogen bond interactions.[12,40] Furthermore, as discussed in section III.A, the IR absorption spectra show water hydroxyls bound to other water molecules. Therefore, even at relatively low water concentration, we analyze the data with the biexponential model embodied in eq 7 because of the existence of sulfoxide−hydroxyl and water−hydroxyl hydrogen bonds.

The amplitudes, A_i, of each fraction provide information about the relative populations of the two types of species. By species here we are referring to the two populations of water−hydroxyl interactions. Figure 3 plots the amplitudes of the 1.8 ps time constant component (water bound to water) as a function of water concentration at four wavelengths across the spectrum. (The amplitude of the water−water component will be referred to as A_w and the water−DMSO component, A_D. $A_w + A_D = 1$.) While there is scatter in the data as a function of wavelength, there is a consistent trend. As the wavelength moves to the red, A_w becomes larger. This is consistent with a two-component model, and the spectra are shown in Figure 1. As the wavelength is shifted to the red, the spectrum will have an increased absorption due to ODs bound to water oxygens and a decreased absorption from ODs bound to DMSO oxygens. A_w is quite small in the low water concentration solutions and only increases substantially after a DMSO:water ratio of n = 1:1 (X = 0.5).

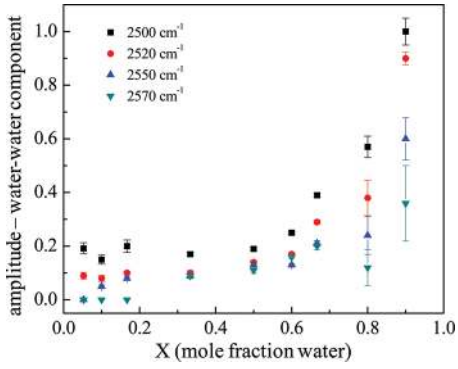

Figure 3. Fractional amplitudes of the water−water component lifetime, A_w, are given for various wavelengths as a function of the water mole fraction, X_{H_2O}, in the water−DMSO solutions.

Figure 3 demonstrates two main trends: an A_w dependence on water concentration and, for a given concentration, an A_w dependence on wavelength. The population information contained in relative amplitudes A_w and A_D as a function of water concentration are in accord with structural findings from the MD simulations of Borin and Skaf.[25] As mentioned in the Introduction, in solutions with less than 50% water the MD simulations show a dominance of configurations in which one water molecule bridges two DMSO molecules. There are also some instances of a water hydrogen bonding to the oxygen of a bridging water molecule (see Figure 4). The large A_D values in these solutions confirms that much of water's interactions occur with DMSO. Furthermore, we find a small but significant population of water−water interactions exist in solutions with water concentrations much less than 50%, that is, solutions containing 18:1 and 9:1 DMSO:water, in contrast to what would occur if water molecules were randomly distributed in the water/DMSO solutions.

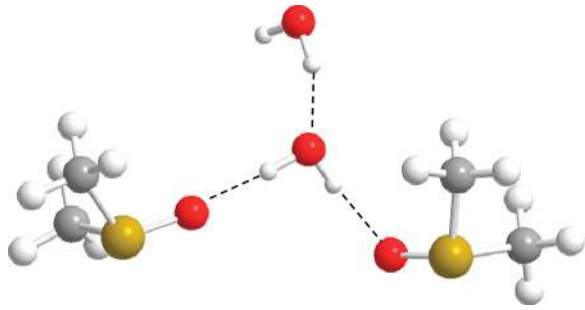

Figure 4. A water hydrogen bonded bridging two DMSO molecules with a second water hydrogen bonded to the bridging water oxygen. The figure was adapted from a snapshot taken from an MD simulation by Borin et al.[25]

This trend in population amplitude can be explained by looking at species formed by water's concentration-dependent interactions. MD simulations[25] suggest the existence of three main species. The first are water molecules bridging two DMSO molecules which we refer to as DW. These are first order in water concentration meaning only one water molecule is necessary for DW to form. This species has a lifetime longer than bulk water. The second species is a water hydroxyl bound to the water oxygen of a DW (Figure 4). This hydroxyl has the 1.8 ps lifetime. We will refer to these as DWW. The other type of structure is two water hydroxyls hydrogen bonded to a single DMSO oxygen. There are a variety of ways this can occur, but the lifetime will be long compared to that of an OD hydrogen bonded to a water oxygen. We will call these WDW. DWW and WDW are second order in water, meaning that these species require two water molecules to form.

Because DWW and WDW are second order in the water concentration, at extremely low water concentrations, virtually only DWs will exist. At relatively low water concentrations (18:1; 9:1), the second-order species (DWW and WDW) will start to grow in concentration faster than the first-order species (DW). In Figure 3, A_w only gradually increases with increasing water concentration up to X = 0.5 (n = 1:1) because both DWW and WDW are second order in the water concentration, but only DWW has the short lifetime that gives rise to A_w. Above X = 0.5, A_w increases rapidly. While DW and WDW structures become saturated, there is no limit to the number of structures with a hydroxyl hydrogen bonded to a water oxygen. Such structures include the DWW structures, but at higher water concentrations, there will also be bulklike water networks in which hydroxyls are bound to water oxygens. The result is that A_w will approach 1 at very high water concentration.

dx.doi.org/10.1021/jp301967e | J. Phys. Chem. B 2012, 116, 5479−5490

Values for the long decay time constant as a function of water concentration are shown in Figure 5. As the water concentration increases, the long time constant becomes shorter. Though in the discussion above we combined the DW and WDW structures within a long-lifetime component A_D, these two structures are unlikely to give rise to the same lifetime. In addition, as the water concentration increases, both species will have their water oxygens become hydrogen bond acceptors for water hydroxyls changing the lifetime of the hydroxyl hydrogen bonded to the DMSO oxygen. Therefore, as the water concentration is increased, the hydroxyls bound to the DMSO oxygens experience an increase in local structural complexity which provides more pathways for relaxation of the excited OD hydroxyl stretch. The range of acceptor modes and the density of states will increase. Such changes are the probable explanation for the decrease in the long lifetime with increasing water concentration shown in Figure 5.

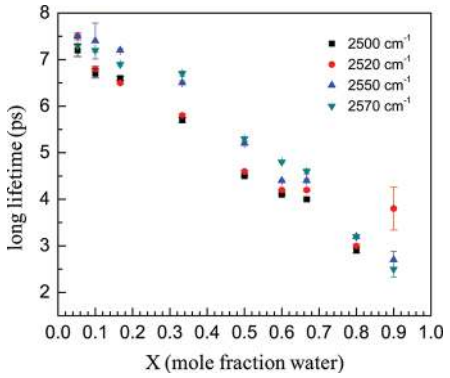

Figure 5. The longer population decay time (lifetime) for water bound to DMSO for various wavelengths as a function of X_{H_2O}, the mole fraction of water in solution.

C. Orientation Dynamics from IR Pump−Probe and OHD-OKE Measurements. Figure 6 displays $r(t)$, the anisotropy decays (orientational relaxation) for several samples at 2550 cm^{-1}. The data exhibit biexponential behavior with an initial fast decay of small amplitude followed by a slower, large amplitude component. Figure 6 demonstrates a general trend among the samples. In the figure, n = 18:1 and 5:1 samples have anisotropies which decay on similar time scales. When the water concentration is increased to an intermediate concentration (Figure 6, n = 1:2), the anisotropy decays more slowly. We observe biexponential decays in samples with water concentration as high as n = 1:4. The n = 1:9 sample is different. It has a fast initial decay that becomes very slow that appears to be leveling off. The dynamics are not biexponential and will be discussed separately below.

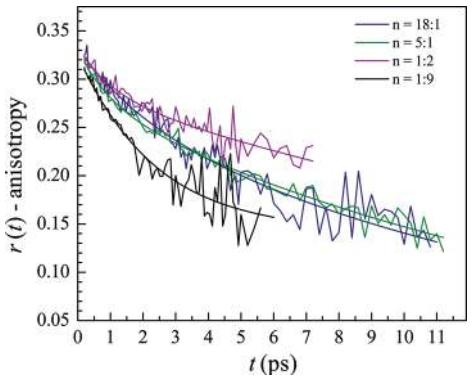

Figure 6. Examples of anisotropy decays from water/DMSO solutions of specified DMSO:water ratios, n, at 2550 cm^{-1}. The anisotropy decays are the water orientational relaxation.

With the exception of the n = 1:9 sample, the anisotropy decays were fit to biexponentials within the framework of eq 4.

$$r(t) = A_1^{or} e^{-t/\tau_1^{or}} + A_2^{or} e^{-t/\tau_2^{or}} \quad (8)$$

where A_1^{or} and A_2^{or} are the amplitudes of each component and τ_1^{or} and τ_2^{or} are the decay time constants with $\tau_1^{or} < \tau_2^{or}$. The "or" superscript denotes orientational.

In pure bulk water, complete orientational relaxation involves the concerted dynamics of many molecules because any given water molecule is restricted by its hydrogen bonds to other water molecules.[56,57] Here, there are a combination of DMSO molecules and other water molecules in all but the highest water concentration studies. Only the n = 1:9 sample contains sufficient water to have a spatially distinct water only subensemble. The lower water content samples are somewhat analogous to very small water pools in small AOT reverse micelles.[12,40] While two vibrational lifetimes are observed, the orientational relaxation does not decay as two separate components because water orientational relaxation is a concerted processes involving many molecules.

As in small AOT reverse micelles,[12,40] the biexponential anisotropy decay observed here is caused by two orientational relaxation mechanisms. The fast decay of small amplitude is assigned to the wobbling-in-a-cone mechanism,[11,35−37] a fast diffusive sampling of a limited range of angles. The observed OD hydroxyl can only sample a limited angular range because it is restricted by its hydrogen bonds. The restricted wobbling of the OD transition dipole contributes to the anisotropy decay but does not result in complete decay of the anisotropy. The slow component of decay is the full orientational randomization of the water molecules, which requires hydrogen bond rearrangements to allow the OD transition dipole to sample all angles.

Using the wobbling-in-a-cone model to describe the fast component of biexponential decay, the observed anisotropy has the function form[11,37]

$$r(t) = [S^2 + (1 - S^2)e^{-t/\tau_{wob}^{or}}]e^{-t/\tau_w^{or}} \quad (9)$$

where S $(0 \le S \le 1)$ is a generalized order parameter that describes the degree of angular cone restriction, τ_{wob}^{or} is the time constant for angular diffusion within the cone, and τ_w^{or} is the time constant for the complete orientational relaxation of water in the water/DMSO systems.

Wobbling parameters can be obtained from a biexponential fit by comparing eqs 8 and 9:

$$S^2 = A_2^{or} \quad (10a)$$

$$\tau_{wob}^{or} = [(\tau_1^{or})^{-1} - (\tau_2^{or})^{-1}]^{-1} \quad (10b)$$

$$\tau_w^{or} = \tau_2^{or} \quad (10c)$$

The cone semiangle, θ_c, can be found by

$$S = 0.5 \cos\theta_c(1 + \cos\theta_c) \quad (11)$$

The wobbling-in-the-cone diffusion constant D_c is in turn related to τ_{wob}^{or} and θ for $\theta \le 30°$ by[35]

dx.doi.org/10.1021/jp301967e | J. Phys. Chem. B 2012, 116, 5479−5490

Table 2. Orientational Parameters from Anisotropy Experiments of OD:Water Time Constant (τ_w^{or}), Wobbling Time Constant (τ_{wob}^{or}), Wobbling Half-Angle (θ_c), and Order Parameter (S); Water Time Constant from Two-Component Fit Given by τ_{w2}^{or}; Time Constant of DMSO Orientational Relaxation (τ_{DMSO}^{or}) from OHD-OKE Experiments

DMSO:water	τ_{w2}^{or} (ps)	τ_{wob} (ps)	θ_c (deg)	S	τ_w^{or} (ps)	τ_{DMSO}^{or} (ps)
18:1		0.6 ± 0.2	27 ± 3	0.53 ± 0.03	14 ± 2	11 ± 1
9:1		1.2 ± 0.8	26 ± 1	0.54 ± 0.01	18 ± 3	13 ± 1.5
5:1		1.7 ± 0 0.4	26 ± 2	0.54 ± 0.02	17 ± 2	14 ± 2
2:1		1 ± 0.3	25 ± 3	0.55 ± 0.03	18 ± 2	18 ± 1.5
1:1		0.6 ± 0.3	25 ± 3	0.55 ± 0.02	20 ± 2	22 ± 2
1:2		1.2 ± 0.3	24 ± 2	0.55 ± 0.02	20 ± 3	23 ± 1
1:4		2.3 ± 0.5	22 ± 1	0.56 ± 0.01	14 ± 4	16 ± 1
1:9	2.8 ± 0.8				12 ± 1	14 ± 2
bulk water					2.6 ± 0.2	

$$D_c \cong 7\theta^2/24\tau_{wob}^{or} \quad (12)$$

with θ in radians. In the experimental systems studied here, $\theta \leq 30°$, and eq 12 applies.

Data at a number of wavelengths for each water concentration were fit with biexponential functions. Within experiment error there is no wavelength dependence. The lack of wavelength dependence is consistent with the physical picture that the orientational relaxation is concerted and involves a number of molecules that determine the orientational relaxation dynamics. This is in contrast to the absorption frequency and the vibrational lifetime which depend principally on the immediate local environment of the OD hydroxyl. Because of the lack of a wavelength dependence for the orientational relaxation, the dynamic data were wavelength averaged for each sample. Table 2 lists the time constants τ_w^{or} and the wobbling parameters, θ_c, S, and τ_{wob}^{or}, as a function of water concentration.

The cone angles are all very similar, ~25°, and essentially independent of water concentration within experimental error with the possible exception of n = 1:4, the highest water content sample for which wobbling is observed. This sample has a slightly smaller cone angle. At room temperature, water molecules have enough energy to sample substantial portions of the hydrogen bond potential energy surface. In MD simulations of pure water, one of the characteristics used to define the existence of a hydrogen bond is that the angle between the O−D bond and the O−O axis is less than 30°.[56] This definition permits a significant amount of orientational space to be sampled without breaking a hydrogen bond. In contrast, a large amplitude change in the orientation of the O−D bond can only be achieved through a rearrangement of the hydrogen bond network by breaking and forming new hydrogen bonds. This is called the jump reorientation mechanism,[56,58] which is discussed further below.

Here we have both water−water and water−DMSO hydrogen bonds. It is reasonable to assume that the same qualitative considerations that apply to pure water also apply here. Therefore, over some range of angles sampled, the orientational motion of the O−D bond will be caused by thermal fluctuations of the intact hydrogen bond network and will be diffusive in nature. The only restriction on the motion of the O−D in this regime is the increase in potential energy as it moves away from the OD---O axis where the second O is either that of a water molecule or a DMSO molecule.

As shown in eq 12, the angular diffusion constant for the wobbling motion depends on both the decay constant and on the cone angle. Because the cone angles are all essentially the same, we can compare the decay constants. Starting with the lowest water concentration (18:1), the decay time becomes longer as the water concentration is increased from the lowest water concentration, although there is significant overlap of the error bars. Over this range of water concentrations, the viscosity is increasing. However, around the n = 1:1 concentration (2:1, 1:1, and 1:2) the wobbling decay constant decreases even though this is the water concentration range with the highest viscosity (see Figure 9A). At still higher water concentration (1:4) the wobbling decay slows substantially. For this water concentration, the cone angle is somewhat smaller, and D_c (see eq 12) is even smaller compared to the value for 1:2 than is given by the change in the decay times. This trend may reflect the effect of changing structure as the system goes from water deficient to water rich, although the large error bars make the trend uncertain.

The highest water concentration sample, n = 1:9, is different from the lower water content samples in that there are two lifetimes and two orientational relaxation times, one for each subensemble of water molecules. One subensemble is comprised of water molecules that interact with or are influenced by DMSO. The other is bulklike water, with only water−water interactions for the particular water with the OD group that is observed and surrounding water molecules. Data analysis of this type of two-component anisotropy decay has been described in detail previously in the context of analyzing water dynamics in AOT reverse micelles and other systems.[9,59] The characteristics of the decay are such that there is a relatively fast decay for the bulklike water followed by what looks like a plateau or a decay approaching a plateau, as in Figure 6. At even longer time, the anisotropy decays to zero. The apparent plateau is produced because the vibrational lifetime is too short to observe the entire decay.[12] In Table 2 for the n = 1:9 sample, these relaxation times are listed as τ_{w2}^{or}, the bulklike water component, and τ_w^{or}, which is the water influenced by the presence of DMSO as in the lower concentration samples. It is worth noting that the decay time τ_{w2}^{or} = 2.8 ± 0.8 ps is the same as the orientational relaxation time of HOD in bulk H_2O, that is, 2.6 ps, within experimental error.[11]

For all of the samples studied, the long time constant τ_w^{or} increases with increasing water concentration until intermediate concentrations (n = 1:2) and then decreases with a further increase in water content (see Table 2). This trend is consistent with that observed by experiments finding a maximum in the orientational relaxation time at intermediate concentrations[21,23,29] but runs counter to experiments that suggest

dx.doi.org/10.1021/jp301967e | J. Phys. Chem. B 2012, 116, 5479−5490

water orientational relaxation times in water/DMSO mixture of ~1 ps.[30,31]

For bulk water, orientational relaxation does not occur through Gaussian angular diffusion (a very large number of very small angular steps).[60] On the basis of their MD simulations of bulk water, Laage and Hynes found that the orientational motions of water molecules are better described by a jump reorientation model based on Ivanov's approach,[58] in which the jumps correspond to the rearrangement of hydrogen bonds among water molecules.[56] Complete orientational relaxation involves the breaking and forming of hydrogen bonds. The mechanism requires the donating hydroxyl to go through a transition coordinate that bisects the outgoing acceptor and an encroaching incoming acceptor. Energetically a water molecule will not break a hydrogen bond without virtually immediately forming a new hydrogen bond.[61]

For water/DMSO solutions, the changes in τ_w^{or} as a function of concentration (Table 2) suggest water dynamics are closely tied to the dynamics and structure of the overall solution. τ_w^{or} generally tracks with concentration-dependent measurements made with dielectric relaxation[23,62] and NMR[21,28,29,63] and with MD simulations.[25] τ_w^{or} also follows the viscosity[17] as discussed below. In the context of the jump reorientation model, gaining access to the new hydrogen bond acceptor is the slow step in the orientational relaxation. At low water concentrations most of the acceptors are DMSO oxygens. A vacant DMSO acceptor will need to reorient to come into a configuration that will permit a hydrogen bonded water hydroxyl to jump to the vacant acceptor. The effect of having more DMSO−water hydrogen bonds in solution decreases acceptor accessibility by tying up DMSO oxygens. This lack of acceptors will be greatest at intermediate water concentrations. As the water concentration is increased further, an increasing number of water oxygens become available as acceptors.

In addition, at low water concentration, the DMSOs not directly interacting with water molecules have weak interactions that do not result in one distinct structure. Neutron diffraction studies show that liquid DMSO contains neither highly specific interactions nor one well-defined structure,[64] while Raman studies have inferred both antiparallel and linear DMSO arrangements.[22] Bulk water MD simulations have shown that the mobility of single water molecules and bulk water's ability to quickly reorient depend on defects in the tetrahedral network, providing low-energy pathways to reorientation.[65] While the tetrahedral structure of the DMSO:water network is similar to bulk water, a more ordered hydrogen bond network as well as steric interactions from methyl groups would impede mobility and provide fewer pathways for jump reorientation and exchange. This picture says that the rate of water orientational relaxation is directly tied to the rate of DMSO orientational relaxation. Only at very high water concentration will there be enough water acceptors to allow some water orientational relaxation to depend on the motion of other water molecules rather than on the reorientation of DMSO. In the systems studied here, only the n = 1:9 is in this high water concentration regime.

To test that water's reorientation dynamics are tied to those of DMSO, the orientational relaxation of DMSO was measured using OHD-OKE experiments. As mentioned above, the OHD-OKE experiments measure the anisotropic component of the polarizability−polarizability correlation function. At all but the shortest times, the polarizability−polarizability correlation function is the same as the orientational correlation function (second Legendre polynomial correlation function).[66,67] The strength of the signal in a OHD-OKE experiment depends on the molecular polarizability and polarizability anisotropy. DMSO is both highly polarizable and has a relatively large polarizability anisotropy. In contrast, both water's polarizability and polarizability anisotropy are small. Previous studies found that there was no contribution to the intermolecular OKE signal from water in DMSO/water mixtures until the mole fraction of DMSO was <0.05.[31] Our studies are in accord with this and indicate that even in our highest water concentration sample (DMSO mole fraction of 0.1) there is at most a small contribution to the signal from the water.

Studies of a wide variety of liquids using OHD-OKE experiments show generally that the initial decay of the signal consists of several power laws that reflect "caging" of one molecule by the surrounding molecules.[68,69] The power law decays are followed by the complete orientational relaxation that randomizes the orientations.[69] Mode coupling theory (MCT) can be used to describe the data.[68−70] While we are interested in the final long time exponential decay that is associated with the randomization of the orientation, it is necessary to fit the data globally, including the power laws, to accurately extract the final exponential decay. While the mode coupling description of the decays does not produce analytical results, it has been demonstrated that a model fitting function that mimics the MCT results can be used to fit the data and extract the different time components.[45,70]

$$y(t) = (at^{-b} + ct^{-d})e^{-t/\tau_{DMSO}^{or}} \quad (13)$$

where a, b, c, and d are power law fit parameters and τ_{DMSO}^{or} is the orientational relaxation time constant of DMSO.

Figure 7 shows representative OHD-OKE curves with fits (red dashed curves) to eq 13. The data are displayed on a log plot. The small oscillations at short time are caused by excitation of intramolecular vibrations and have been studied in detail.[31] At ~10 ps, the data begin to bend over. This longer time part of the curve is the exponential decay. The orientation relaxation times (the exponential decay constants) τ_{DMSO}^{or} are listed in the last column of Table 2 and should be compared to the value of τ_w^{or}, which are also listed in the table. Figure 8 plots τ_{DMSO}^{or} and τ_w^{or} as a function of water mole fraction, X_{H_2O}. The dashed curve is an aid to the eye. Although the agreement between τ_{DMSO}^{or} and τ_w^{or} is not perfect, given the error bars the two sets of data demonstrate that the orientational relaxation of

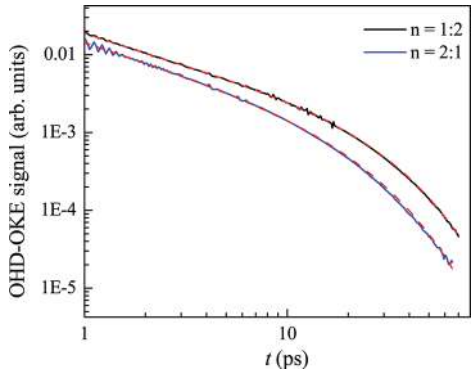

Figure 7. Examples of OHD-OKE curves for DMSO:water ratios, n, 2:1 and 1:2. The decay as the DMSO orientational relaxation. Note the data are on a log plot.

dx.doi.org/10.1021/jp301967e | J. Phys. Chem. B 2012, 116, 5479−5490

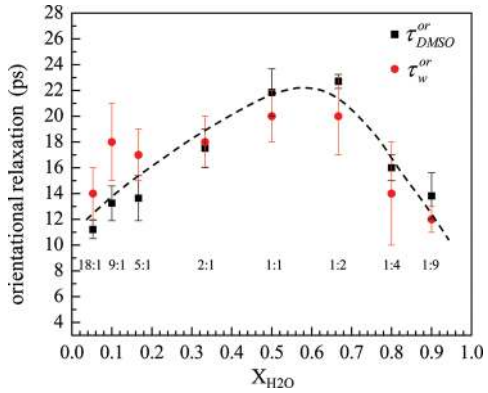

Figure 8. Comparison of the anisotropy IR pump−probe water slow orientational time constant (τ^{or}_{w}) and OHD-OKE DMSO orientational time constant (τ^{or}_{DMSO}) as a function of water mole fraction. The two types of data are almost the same within experimental error and display the identical trend. The numbers below the points are n = DMSO:water. The dashed line is an aid to the eye.

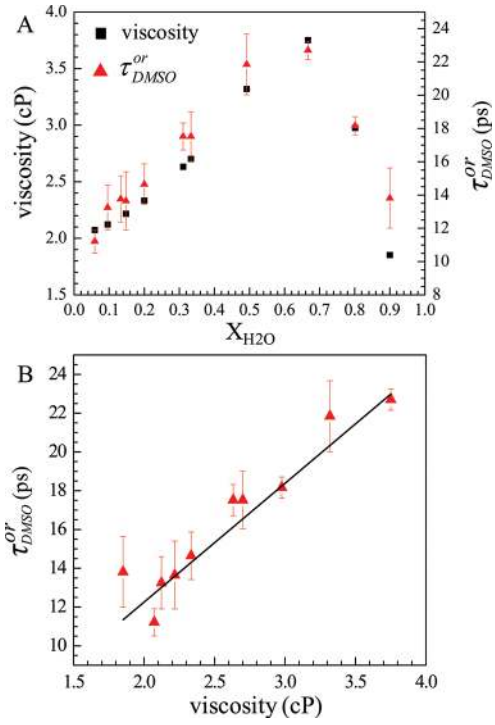

Figure 9. (A) Comparison of the viscosity (left vertical axis) and τ^{or}_{DMSO} (right vertical axis) as a function of water mole fraction. (B) τ^{or}_{DMSO} vs viscosity. The line through the data is the best linear fit. Within experimental error, the DMSO orientational relaxation time track the viscosity even though the viscosity is not monotonic. Viscosity data are from Cowie et al.[17]

water measured with the IR pump−probe experiments is almost the same as the orientational relaxation of DMSO measured with the OHD-OKE experiments. These results support the concerted jump reorientation model for the water orientational relaxation in the DMSO mixtures. A water molecule can undergo fast wobbling motions, but to completely randomize its orientation requires the rotation of a DMSO into a configuration to provide a new acceptor for the water hydroxyl to jump to.

Figure 9 shows the relationship between the DMSO orientational relaxation time, τ^{or}_{DMSO}, and the viscosity. In Figure 9A, the viscosity (left vertical axis) is plotted vs the water mole fraction, X_{H_2O}. The right vertical axis is the orientational relaxation time. With the exception of the highest water concentration point, the viscosity and the orientational relaxation are very well correlated. Figure 9B shows τ^{or}_{DMSO} vs viscosity. The line is the best linear fit to the data. The data closely approximate a line, which indicates that the orientational relaxation of the DMSO is hydrodynamic in spite of the fact that the viscosity does not increase monotonically.

D. 2D IR Vibrational Echo Measurements of Spectral Diffusion. Figure 10 shows 2D IR vibrational echo spectra taken at three T_ws for a low water concentration (n = 9:1) and an intermediate water concentration (n = 1:2). The red bands are positive going and arise from the v = 0 to the v = 1 OD stretch vibrational transition. The blue bands are negative going and are produced by vibrational echo emission at the 1−2 vibrational transition. The difference in the center-to-center frequency of the two bands along the ω_m axis (vertical axis) is the anharmonicity of the OD stretching mode. At the shortest time, the 0−1 band is substantially elongated along the diagonal (dashed line in upper left panel). The elongation results from inhomogeneous broadening. A given vibrational oscillator has not sampled all frequencies (structures). As time progresses, the shapes of the bands become progressively less elongated as the oscillator samples more and more frequencies. The sampling of frequencies is caused by the OD oscillators experiencing changing interactions caused by structural changes. For the n = 9:1 data (left panels), by 8 ps the 0−1 band is almost round, which shows that almost all frequencies within the vibrational absorption line have been sampled (spectral diffusion), which means that almost all liquid structures have been sampled. In contrast, the n = 1:2 spectrum at 8 ps is still significantly elongated along the diagonal, which shows that spectral diffusion is slower in this sample than in the n = 9:1 solution.

The FFCF parameters in Table 3 show trends with changing water concentration. The homogeneous line width, Γ, increases with increasing water concentration while τ_1 and τ_2 increase as the water concentration is increased and then decrease again at high water concentrations. As observed in the water/DMSO systems studied here, MD simulations of pure bulk water when compared to the 2D IR found three time scales governing the FFCF of bulk water in both the experiments and simulations.[71,72] In bulk water, the homogeneous component results from extremely fast (tens of femtoseconds) local fluctuations mainly in hydrogen bond length that result in motional narrowing and give rise to the pure dephasing component of the absorption line. The slowest time scale component (τ_2) involves global rearrangement and randomization of the hydrogen bond structure. The intermediate decay component (τ_1) was interpreted as a transition between the very small local motions and complete structural randomization. Similar processes on different time scales were found in simulations[73] of 2D IR vibrational echo experiments[5] of water/NaBr solutions. The simulations show that while the FFCF decay on fast time scales is due to different local mechanisms than in pure water, the longest time scale component is indicative of a global rearrangement of hydrogen bonds and complete randomization of the liquid structure. Like pure water, the DMSO:water solutions' FFCFs also have three terms: a homogeneous component and fast and slow decay

dx.doi.org/10.1021/jp301967e | J. Phys. Chem. B 2012, 116, 5479−5490

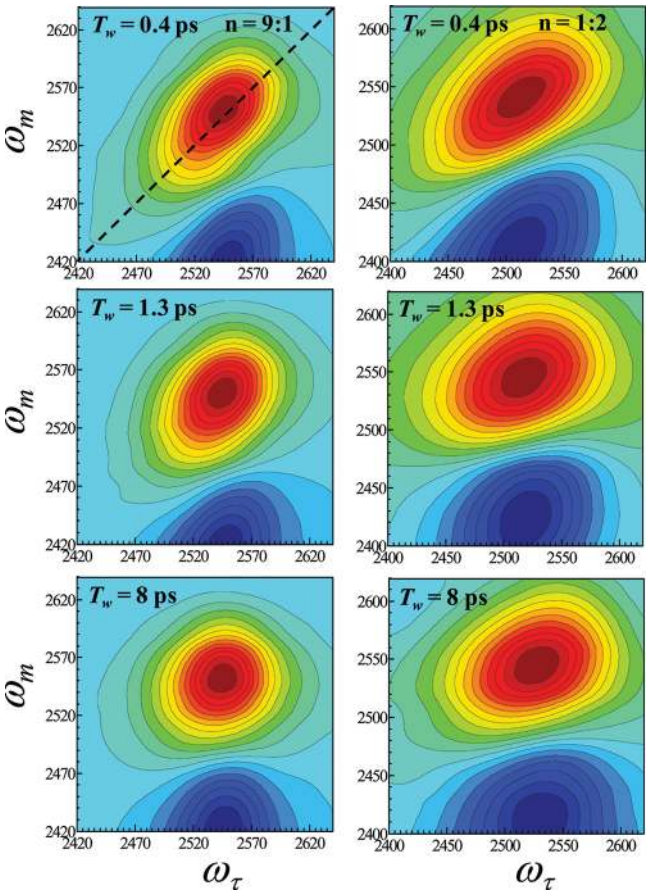

Figure 10. Examples of 2D IR vibrational echo spectra of the OD stretch at n = 9:1 and n = 2:1 DMSO:water at several times. As T_w increases, the shapes of the bands change due to spectral diffusion. Analysis of the time-dependent shape changes gives the time dependence of the structural evolution of the water−DMSO solutions.

terms. It is reasonable to discuss the current results in light of the interpretations of the water simulation results.

The homogeneous line width, Γ, increases as the water concentration increases. However, it is interesting to note that the ratios of the Γs to the corresponding total absorption line widths (Table 1) are invariant with water concentration and the same as that of bulk water within experimental error. As the water concentration is increased, the total absorption line width increases, demonstrating that there are a wider range of structures experienced by the OD hydroxyl stretch. The same fraction of the increased number of structures is sampled on the ultrafast time scale, giving rise to the proportional homogeneous component of the absorption line.

τ_1 and τ_2 in Table 3 are the time constants associated with spectral diffusion. These should be viewed as characteristic time scales and not representative single well-defined processes. Both time constants increase as the water concentration is increased and then decrease at high water concentration. The long time component, τ_2, corresponds to the time for complete sampling of the inhomogeneous vibrational absorption line. The OD hydroxyl stretch frequency shift from its gas phase value is principally determined by its hydrogen bonding.[46] Therefore, the slowest component of the spectral diffusion reflects the final complete sampling of all hydrogen bonding structures. Then in analogy to bulk water, the faster component of the spectral diffusion, τ_1, is associated with more limited motions that influence the nature of the hydrogen bonds.

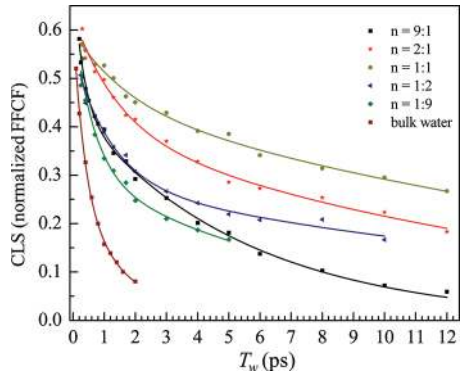

Figure 11. CLS curves obtained from analysis of the 2D IR spectra like those shown in Figure 10 for several values of n = DMSO:water. The CLS curves are the normalized frequency−frequency correlation function. Combined analysis of the CLS curves and the absorption spectra gives the full frequency−frequency correlation function.

The trend in the τ_2 value is similar to that seen in the orientational relaxation. Even at the highest water concentration, n = 1:9, the spectral diffusion is ∼3 times slower than that of pure water. Spectral diffusion is not complete until all structural configurations are sampled. In the water/DMSO mixture, that cannot occur until all initial DMSO configurations randomize. At high water concentration, at least some of the water molecules will have a DMSO as one of its hydrogen bonding partners, and rearrangement of such structures is slow because of the size of the DMSO compared to the situation in pure water. For the intermediate water concentration samples, the spectral diffusion is ∼4 times slower than that of the highest and lowest water concentration samples. This slowing is most likely caused by the presence of well-defined water−DMSO hydrogen bonding structures resulting in the inhibition of

Table 3. FFCF Fit Parameters of the DMSO−Water Binary Mixtures

DMSO:water	T_2 (ps)	Γ (cm^{-1})	Δ_1 (cm^{-1})	τ_1 (ps)	Δ_2 (cm^{-1})	τ_2 (ps)
9:1	0.24	45 ± 3	18 ± 3	0.4 ± 0.5	23 ± 2	6 ± 1
5:1	0.23	46 ± 5	21 ± 2	0.8 ± 0.5	19 ± 2	7 ± 1
2:1	0.22	49 ± 8	22 ± 3	1.4 ± 0.4	29 ± 5	16 ± 3
1:1	0.19	55 ± 4	20 ± 2	1.7 ± 0.7	35 ± 2	23 ± 2
1:2	0.17	64 ± 6	30 ± 3	1.2 ± 0.3	28 ± 3	21 ± 6
1:4	0.17	63 ± 6	43 ± 2	1.7 ± 0.7	28 ± 3	8 ± 5
1:9	0.15	70 ± 8	34 ± 4	0.6 ± 0.4	40 ± 3	6 ± 1
bulk water[a]	0.14	76 ± 14	41 ± 8	0.4 ± 0.08	34 ± 11	1.7 ± 0.2

[a]Data from Park et al.[5]

dx.doi.org/10.1021/jp301967e | J. Phys. Chem. B 2012, 116, 5479−5490

hydrogen bond rearrangement as discussed in connection with the orientational relaxation.

The comparison between the slowest component of the water orientational relaxation and the slowest component of the spectral diffusion is informative. The times measured in the two types of experiments cannot be directly compared because the experiments measure different correlation functions, that is, the FFCF for the vibrational echoes and the second Legendre polynomial correlation function for the orientational relaxation. Nonetheless, the two observables are related because their time dependencies are controlled by similar processes. In pure bulk water, the slowest component of the FFCF is 1.7 ps[71,72] and the orientational relaxation time is 2.6 ps.[11,74]

Looking at Tables 2 and 3, it is seen that for the highest water content sample, n = 1:9, both τ_w^{or} (12 ps) and τ_2 (6 ps) are substantially slower than the corresponding values for bulk water, 2.6 and 1.7 ps, respectively. Thus, even at this relatively high water concentration, the water/DMSO mixture still has dynamics that are far from those of bulk water. In the lowest water concentration water/DMSO mixtures, both τ_w^{or} and τ_2 are relatively fast, become significantly slower at intermediate water concentrations, and then become faster again as the water concentration increases further. Both τ_w^{or} and τ_2 are the slowest in the water concentration range n = 2:1, 1:1, and 1:2. This is the concentration range in which most DMSO oxygens have two hydroxyls hydrogen bonded to them, but not yet so high that there is a large fraction of the water molecules interacting with other water molecules that are not hydrogen bonded to DMSO. At n = 1:1, there would be just enough water hydroxyls to make two hydrogen bonds to each DMSO oxygen. However, both the absorption spectra and the lifetime measurements show that there are some water−water hydrogen bonds in addition to water−DMSO hydrogen bonds. Because τ_2 is indicative of global structural reorganization, it is not surprising that the anisotropy data obtained through pump−probe and OHD-OKE experiments track well with the long time constant of the FFCF.

IV. CONCLUDING REMARKS

The 2D IR vibrational echo experiments of the hydroxyl stretch (OD of dilute HOD in H_2O/DMSO) provide a detailed view of the dynamics of water in water/DMSO mixtures. The results give the time scales for all types of structural changes and also decompose the absorption spectrum into its underlying homogeneous and inhomogeneous components. In analogy to pure water, the homogeneous and very fast dynamics (Γ and τ_1 in Table 3) are ascribed to very local structural fluctuations mainly associated with hydrogen bond length and small angular changes. The slower time scale dynamics (τ_2 in Table 3) are the complete frequency randomization and, therefore, the complete structural randomization of the hydrogen bonding network. These dynamics are fast at both low and high water concentrations but slow substantially at intermediate water concentrations.

Polarization-sensitive IR pump−probe experiments were used to determine the population and orientational relaxation of water. Biexponential population relaxation data combined with the absorption spectra show that water hydroxyls hydrogen bond to two different acceptors: DMSO oxygens and water oxygens even at quite low water concentration. The pump−probe anisotropy results showed that water undergoes orientational relaxation on two time scales for all but the highest water concentration. The fast time scale is caused by restricted angular motions within a limited cone of angles (wobbling-in-a-cone). The longer time scale represents a collective orientational relaxation of the entire ensemble. Like the slowest dynamical component measured in the 2D IR experiments, τ_w^{or} is faster at low and high water concentrations and slower at intermediate water concentrations.

In the water−DMSO mixtures, the complete orientational relaxation occurs in ∼10 to ∼20 ps depending on the water concentration. We proposed that the limiting step in the orientational relaxation of water is the reorientation of DMSO molecules to bring them into the correct configuration to accept the hydroxyl hydrogen bond donor. To test this hypothesis, optical heterodyne detected optical Kerr effect measurements were performed that directly measure the orientational relaxation times, τ_{DMSO}^{or}, of DMSO in the water−DMSO mixtures (see Table 2). Within experimental error, the DMSO orientational relaxation times and the water relaxation times are the same at all water concentrations. This is strong support for the basic picture of how water undergoes orientational relaxation in water−DMSO solutions. In addition, while the 2D IR experiments and the orientational relaxation experiments do not measure the same correlation function and therefore cannot be directly compared, both are related to the complete structural randomization of the liquid. Comparing the values of τ_w^{or} (Table 2) and τ_2 (Table 3), it can be seen that the times are similar as is the trend with water concentration, providing further support for the model of structural evolution in water−DMSO solutions.

AUTHOR INFORMATION

Corresponding Author

*E-mail: fayer@stanford.edu.

Present Addresses

[†]Current Address: Department of Chemistry, The Hashemite University, Zarqa, Jordan.

[‡]Current Address: Lincoln Laboratory, Massachusetts Institute of Technology, Lexington, MA 02420.

Notes

The authors declare no competing financial interest.

ACKNOWLEDGMENTS

We thank the Department of Energy (DE-FG03-84ER13251) for support of the IR experiments (Daryl B. Wong, Musa I. El-Barghouthi, Emily E. Fenn, Chiara H. Giammanco, and Michael D. Fayer) and the National Science Foundation (DMR 0652232) for support of the OHD-OKE experiments (Kathleen P. Sokolowsky, Adam L. Sturlaugson, and Michael D. Fayer). D.B.W. and K.P.S. thank Stanford for Graduate Research Fellowships. M.E.B. thanks the Fulbright Scholar Program for a Professorial Fellowship.

REFERENCES

(1) Eisenberg, D.; Kauzmann, W. *The Structure and Properties of Water*; Oxford University Press: London, 1969.

(2) Marechal, Y. *The Hydrogen Bond and the Water Molecule: The Physics and Chemistry of Water, Aqueous and Biomedia*; Elsevier: Amsterdam, The Netherlands, 2007.

(3) Ball, P. *Chem. Rev.* **2008**, *108*, 74−108.

(4) Moilanen, D. E.; Wong, D.; Rosenfeld, D. E.; Fenn, E. E.; Fayer, M. D. *Proc. Natl. Acad. Sci. U. S. A.* **2009**, *106*, 375−380.

(5) Park, S.; Fayer, M. D. *Proc. Natl. Acad. Sci. U. S. A.* **2007**, *104*, 16731−16738.

(6) Bakker, H. J. *Chem. Rev.* **2008**, *108*, 1456−1473.

(7) Tielrooij, K. J.; van der Post, S. T.; Hunger, J.; Bonn, M.; Bakker, H. J. *J. Phys. Chem. B* **2011**, *115*, 12638−12647.
(8) Laage, D.; Hynes, J. T. *Proc. Natl. Acad. Sci. U. S. A.* **2007**, *104*, 11167−11172.
(9) Fenn, E. E.; Moilanen, D. E.; Levinger, N. E.; Fayer, M. D. *J. Am. Chem. Soc.* **2009**, *131*, 5530−5539.
(10) Rezus, Y. L. A.; Bakker, H. J. *Proc. Natl. Acad. Sci. U. S. A.* **2006**, *103*, 18417−18420.
(11) Moilanen, D. E.; Fenn, E. E.; Wong, D.; Fayer, M. D. *J. Phys. Chem. B* **2009**, *113*, 8560−8568.
(12) Moilanen, D. E.; Fenn, E. E.; Wong, D.; Fayer, M. D. *J. Chem. Phys.* **2009**, *131*, 014704.
(13) Fenn, E. E.; Wong, D. B.; Fayer, M. D. *Proc. Natl. Acad. Sci. U. S. A* **2009**, *106*, 15243−15248.
(14) Lovelock, J. E.; Bishop, M. W. H. *Nature* **1959**, *183*, 1394−1395.
(15) Farrant, J. *Nature* **1965**, *205*, 1284−1287.
(16) Schichman, S. A.; Amey, R. L. *J. Phys. Chem.* **1971**, *75*, 98−102.
(17) Cowie, J. M. G.; Toporowski, P. M. *Can. J. Chem.* **1961**, *39*, 2240−2243.
(18) Catalan, J.; Diaz, C.; Garcia-Blanco, F. *J. Org. Chem.* **2001**, *66*, 5846−5852.
(19) Soper, A. K.; Luzar, A. *J. Chem. Phys.* **1992**, *97*, 1320−1331.
(20) Soper, A. K.; Luzar, A. *J. Phys. Chem.* **1996**, *100*, 1357−1367.
(21) Wulf, A.; Ludwig, R. *ChemPhysChem* **2006**, *7*, 266−272.
(22) Sastry, M. I. S.; Singh, S. *J. Raman Spectrosc.* **1984**, *15*, 80−85.
(23) Lu, Z.; Manias, E.; Macdonald, D. D.; Lanagan, M. *J. Phys. Chem. A* **2009**, *113*, 12207−12214.
(24) Luzar, A.; Chandler, D. *J. Chem. Phys.* **1993**, *98*, 8160−8173.
(25) Borin, I. A.; Skaf, M. S. *J. Chem. Phys.* **1999**, *110*, 6412−6420.
(26) Vishnyakov, A.; Lyubarsev, A. P.; Laaksonen, A. *J. Phys. Chem. A* **2001**, *105*, 1702−1710.
(27) Ludwig, R.; Farrar, T. C.; Zeidler, M. D. *J. Phys. Chem.* **1994**, *98*, 6684−6687.
(28) Gordalla, B. C.; Zeidler, M. D. *Mol. Phys.* **1986**, *59*, 817−828.
(29) Gordalla, B. C.; Zeidler, M. D. *Mol. Phys.* **1991**, *74*, 975−984.
(30) Cabral, J. T.; Luzar, A.; Teixeira, J.; Bellissentfunel, M. C. *J. Chem. Phys.* **2000**, *113*, 8736−8745.
(31) Wiewior, P. P.; Shirota, H.; Castner, E. W. *J. Chem. Phys.* **2002**, *116*, 4643−4654.
(32) Woutersen, S.; Bakker, H. J. *Nature* **1999**, *402*, 507−509.
(33) Gaffney, K. J.; Piletic, I. R.; Fayer, M. D. *J. Chem. Phys.* **2003**, *118*, 2270−2278.
(34) Corcelli, S.; Lawrence, C. P.; Skinner, J. L. *J. Chem. Phys.* **2004**, *120*, 8107.
(35) Lipari, G.; Szabo, A. *Biophys. J.* **1980**, *30*, 489−506.
(36) Wang, C. C.; Pecora, R. *J. Chem. Phys.* **1980**, *72*, 5333−5340.
(37) Tan, H.-S.; Piletic, I. R.; Fayer, M. D. *J. Chem. Phys.* **2005**, *122*, 174501−174509.
(38) Steinel, T.; Asbury, J. B.; Corcelli, S. A.; Lawrence, C. P.; Skinner, J. L.; Fayer, M. D. *Chem. Phys. Lett.* **2004**, *386*, 295−300.
(39) Asbury, J. B.; Steinel, T.; Stromberg, C.; Gaffney, K. J.; Piletic, I. R.; Fayer, M. D. *J. Chem. Phys.* **2003**, *119*, 12981−12997.
(40) Fenn, E. E.; Wong, D. B.; Fayer, M. D. *J. Chem. Phys.* **2011**, *134*, 054512.
(41) Tokmakoff, A. *J. Chem. Phys.* **1996**, *105*, 1−12.
(42) Park, S.; Kwak, K.; Fayer, M. D. *Laser Phys. Lett.* **2007**, *4*, 704−718.
(43) Kwak, K.; Rosenfeld, D. E.; Fayer, M. D. *J. Chem. Phys.* **2008**, *128*, 204505.
(44) Kwak, K.; Park, S.; Finkelstein, I. J.; Fayer, M. D. *J. Chem. Phys.* **2007**, *127*, 124503.
(45) Sturlaugson, A. L.; Fruchey, K. S.; Fayer, M. D. ASAP 2012.
(46) Pimentel, G. C.; McClellan, A. L. *Annu. Rev. Phys. Chem.* **1971**, *22*, 347−385.
(47) Lawrence, C. P.; Skinner, J. L. *J. Chem. Phys.* **2002**, *117*, 8847−8854.
(48) Scheiner, S. *Hydrogen Bonding: A Theoretical Perspective*; Oxford University Press: New York, 1997.
(49) Hobza, P.; Havlas, Z. *Chem. Rev.* **2000**, *100*, 4253−4264.
(50) Hermansson, K. *J. Phys. Chem. A* **2002**, *106*, 4695−4702.
(51) Joseph, J.; Jemmis, E. D. *J. Am. Chem. Soc.* **2007**, *129*, 4620−4632.
(52) Ashihara, S.; Huse, N.; Espagne, A.; Nibbering, E. T. J.; Elsaesser, T. *J. Phys. Chem. A* **2007**, *111*, 743−746.
(53) Oxtoby, D. W. *Annu. Rev. Phys. Chem.* **1981**, *32*, 77−101.
(54) Kenkre, V. M.; Tokmakoff, A.; Fayer, M. D. *J. Chem. Phys.* **1994**, *101*, 10618.
(55) Akaike, H. *IEEE Trans. Autom. Control* **1974**, *AC19*, 716−723.
(56) Laage, D.; Hynes, J. T. *Science* **2006**, *311*, 832−835.
(57) Laage, D.; Hynes, J. T. *J. Phys. Chem. B* **2008**, *112*, 14230−14242.
(58) Ivanov, E. N. *Sov. Phys. JETP* **1964**, *18*, 1041−1045.
(59) Moilanen, D. E.; Fenn, E. E.; Wong, D.; Fayer, M. D. *J. Am. Chem. Soc.* **2009**, *131*, 8318−8328.
(60) Ramasesha, K.; Roberts, S. T.; Nicodemus, R. A.; Mandal, A.; Tokmakoff, A. *J. Chem. Phys.* **2011**, *135*, 054509.
(61) Eaves, J. D.; Loparo, J. J.; Fecko, C. J.; Roberts, S. T.; Tokmakoff, A.; Geissler, P. L. *Proc. Natl. Acad. Sci. U. S. A.* **2005**, *102*, 13019−13022.
(62) Kaatze, U.; Pottel, R.; Schafer, M. J. *J. Phys. Chem.* **1989**, *93*, 5623.
(63) Muller, M. G.; Hardy, E. H.; Vogt, P. S.; Bratschi, C.; Kirchner, B.; Huber, H.; Searles, D. J. *J. Am. Chem. Soc.* **2004**, *126*, 4704.
(64) Luzar, A.; Soper, A. K.; Chandler, D. *J. Chem. Phys.* **1993**, *99*, 6836−6847.
(65) Geiger, A.; Kleene, M.; Paschek, D.; Rehtanz, A. *J. Mol. Liq.* **2003**, *106*, 131−146.
(66) Deeg, F. W.; Stankus, J. J.; Greenfield, S. R.; Newell, V. J.; Fayer, M. D. *J. Chem. Phys.* **1989**, *90*, 6893.
(67) Ruhman, S.; Williams, L. R.; Joly, A. G.; Kohler, B.; Nelson, K. A. *J. Phys. Chem.* **1987**, *91*, 2237−2240.
(68) Götze, W.; Sperl, M. *Phys. Rev. Lett.* **2004**, *92*, 105701.
(69) Cang, H.; Li, J.; Andersen, H. C.; Fayer, M. D. *J. Chem. Phys.* **2005**, *124*, 014902.
(70) Sturlaugson, A. L.; Fruchey, K. S.; Lynch, S. R.; Aragon, S. R.; Fayer, M. D. *J. Phys. Chem. B* **2010**, *114*, 5350−5358.
(71) Asbury, J. B.; Steinel, T.; Kwak, K.; Corcelli, S. A.; Lawrence, C. P.; Skinner, J. L.; Fayer, M. D. *J. Chem. Phys.* **2004**, *121*, 12431−12446.
(72) Asbury, J. B.; Steinel, T.; Stromberg, C.; Corcelli, S. A.; Lawrence, C. P.; Skinner, J. L.; Fayer, M. D. *J. Phys. Chem. A* **2004**, *108*, 1107−1119.
(73) Lin, Y.-S.; Auer, B. M.; Skinner, J. L. *J. Chem. Phys.* **2009**, *131*, 144511.
(74) Rezus, Y. L. A.; Bakker, H. J. *J. Chem. Phys.* **2006**, *125*, 144512−144511−144519.